Apoptosis (2019) 24:730–744
https://doi.org/10.1007/s10495-019-01553-9

JNK inhibition blocks piperlongumine-induced cell death and transcriptional activation of heme oxygenase-1 in pancreatic cancer cells

Jiyan Mohammad[1] · Rahul R. Singh[1] · Cody Riggle[1] · Brandon Haugrud[1] · Maher Y. Abdalla[2] · Katie M. Reindl[1]

Published online: 26 June 2019

Abstract

Piperlongumine (PL) is an alkaloid that inhibits glutathione *S*-transferase pi 1 (GSTP1) activity, resulting in elevated reactive oxygen species (ROS) levels and cancer-selective cell death. We aimed to identify stress-associated molecular responses to PL treatment in pancreatic ductal adenocarcinoma (PDAC) cells. GSTP1 directly interacts with JNK, which is activated by oxidative stress and can lead to decreased cancer cell proliferation and cell death. Therefore, we hypothesized that JNK pathways are activated in response to PL treatment. Our results show PL causes dissociation of GSTP1 from JNK; robust JNK, c-Jun, and early ERK activation followed by suppression; increased expression of cleaved caspase-3 and cleaved PARP; and nuclear translocation of Nrf2 and c-Myc in PDAC cells. Gene expression analysis revealed PL caused a > 20-fold induction of heme oxygenase-1 (HO-1), which we hypothesized was a survival mechanism for PDAC cells under enhanced oxidative stress. HO-1 knockout resulted in enhanced PL-induced PDAC cell death under hypoxic conditions. Similarly, high concentrations of the HO-1 inhibitor, ZnPP (10 μM), sensitized PDAC cells to PL; however, lower concentrations ZnPP (10 nM) and high or low concentrations of SnPP both protected PDAC cells from PL-induced cell death. Interestingly, the JNK inhibitor significantly blocked PL-induced PDAC cell death, Nrf-2 nuclear translocation, and HMOX-1 mRNA expression. Collectively, the results demonstrate JNK signaling contributes to PL-induced PDAC cell death, and at the same time, activates Nrf-2 transcription of HMOX-1 as a compensatory survival mechanism. These results suggest that elevating oxidative stress (using PL) while at the same time impairing antioxidant capacity (inhibiting HO-1) may be an effective therapeutic approach for PDAC.

Keywords Apoptosis · GSTP1 inhibitor · Nrf2 · Oxidative stress · SnPP · ZnPP

Introduction

JNK and ERK both belong to the mitogen-activated protein kinase (MAPK) family and regulate cellular processes including cell proliferation, survival, and apoptosis [1, 2]. A range of stimuli including growth factors, cytokines, and oxidative stress activate JNK [3, 4]. Depending on the signal and duration, JNK activation leads to divergent responses, with transient JNK activation promoting cell survival [5] and prolonged JNK activation promoting cell death [6]. Similarly, ERKs are activated by a number of signals including growth factors, cytokines, mitogens, and oxidative stress [7]. Although ERK signaling is primarily known to promote cell proliferation and cell survival, recently it has been well documented that reactive oxygen species (ROS)-induced ERK activation leads to cell cycle arrest and apoptosis in various cells [8–11]. Modulation of these kinase pathways significantly affects tumor growth. Further, the cellular response to MAPK activation is tissue-dependent and influenced by the microenvironment [12].

Piperlongumine (PL) is an alkaloid obtained from the *Piper longum* plant that elevates ROS levels to induce cancer-selective cell death [13, 14]. Reports indicate PL

Electronic supplementary material The online version of this article (https://doi.org/10.1007/s10495-019-01553-9) contains supplementary material, which is available to authorized users.

✉ Katie M. Reindl
katie.reindl@ndsu.edu

[1] Department of Biological Sciences, North Dakota State University, Fargo, ND 58108, USA

[2] Department of Pathology and Microbiology, University of Nebraska Medical Center, Omaha, NE 68198, USA

activates JNK signaling and results in apoptosis in a variety of human cancer cell lines including colorectal [15], breast and prostate [16], and cholangiocarcinoma [17]. Similarly, PL activates ERK signaling and results in cell death in colorectal [18] and hepatocellular carcinoma [19]. We have previously reported that PL inhibits PDAC cell proliferation in vitro and in vivo by enhancing ROS and DNA damage [20]. However, the signaling mechanisms that lead to PDAC cell death are unknown for this agent.

A primary target of PL is glutathione *S*-transferase pi-1 (GSTP1), a phase II enzyme that detoxifies electrophiles by conjugating them to glutathione. In non-stressed cells, GSTP1 binds to JNK1 and inhibits its activity. In an oxidative stress environment, GSTP1 dissociates from JNK, resulting in JNK activation, and subsequent effects on cell survival, apoptosis, and tumorigenesis [21–23]. GSTP1 is overexpressed in a variety of cancer types and has been proposed as a therapeutic target to overcome multidrug resistance [24].

Heme oxygenase-1 (HO-1) is an antioxidant enzyme that is upregulated in response to oxidative stress [25]. We have previously shown that PL treatment of PDAC cells results in a robust increase in HO-1 gene expression [26]. HO-1 catabolizes heme to carbon monoxide, iron, and biliverdin, which is an antioxidant that protects cells from apoptosis [27, 28]. Both JNK [29] and ERK signaling pathways contribute to oxidative stress-induced HO-1 gene expression [30]. Inhibition of HO-1 has been proposed as a target of cancer therapy.

In this study, we investigated the signaling mechanisms that contribute to PL-induced PDAC cell death. We focused on JNK and ERK signaling because both of these pathways are activated in response to oxidative stress [31] and there is evidence that PL alters these pathways in other tumor types [17, 18]. We also evaluated the cytotoxic effects of inhibiting HO-1 activity in the presence of PL. The results from this report suggest PL signals through JNK and ERK to cause PDAC cell death, and inhibition of HO-1 in combination with PL enhances PDAC cell death. Therefore, manipulating the redox balance in PDAC cells is a viable treatment approach.

Materials and methods

Reagents

Piperlongumine (PL) was purchased from Indofine Chemical Company. PL was dissolved in 100% DMSO at a stock concentration of 100 mM and diluted in medium to working concentrations. SP600125 and zinc (II) protoporphyrin IX (ZnPP) were purchased from Sigma-Aldrich, and tin protoporphyrin IX (SnPP) was purchased from Enzo. All antibodies and U0126 were purchased from Cell Signaling Technologies. The CellTox™ Green assay was purchased from Promega. A co-immunoprecipitation kit, GST activity fluorescent assay, RNA extraction kits, and nuclear extraction kits were purchased from Thermo Fisher Scientific.

Cell culture

PDAC cell lines (MIA PaCa-2 and PANC-1) were purchased from the American Type Culture Collection and grown at 37 °C with 5% CO_2. MIA PaCa-2 cells were cultured in DMEM high-glucose medium (Thermo Fisher Scientific) supplemented with 10% fetal bovine serum (Atlanta Biologicals), 2.5% horse serum (Corning), and 1% antibiotic/antimycotic solution (penicillin, streptomycin, amphotericin B; Hyclone). PANC-1 cells were cultured in DMEM high-glucose medium supplemented with 10% fetal bovine serum and 1% antibiotic/antimycotic solution. The cell lines were sub-cultured by enzymatic digestion with 0.25% trypsin/1 mM EDTA solution (Thermo Fisher Scientific) when they reached approximately 70% confluency.

Cell toxicity assay

PANC-1 cells and MIA PaCa-2 (5000 cells/well) were seeded in 96-well black plates. After 24 h, cells were treated with different concentrations of PL (0–100 µM) for 72 h. A cell toxicity assay was performed by adding 100 µL of the CellTox™ Green Reagent (2X) to each well and incubating the plates for 15 min at room temperature in dark. The fluorescence was measured at 490 nm excitation and 525 nm emission. The data represent the average ± standard deviation for three independent experiments.

Co-immunoprecipitation assay

The assay was performed according to the manufacturer's instructions. Briefly, PANC-1 cells were treated with 10 µM of PL for 24 h and cells were lysed with 100 µL of 1X lysis solution supplemented with 1% protease and phosphatase inhibitors. The total cell lysates were centrifuged at 13,000×*g* for 5 min to pellet the insoluble material. Total protein (100 µg) was incubated with 25 µL of agarose beads immobilized with JNK antibody and immunoprecipitation was performed by gentle rocking at RT for 2 h. After incubation, the agarose beads were centrifuged at 800×*g* for 1 min, washed 3 times with lysis buffer (200 µL), and each wash was followed by a 1-min centrifugation at 800×*g*. After the final wash, the beads were eluted using 50 µL of elution buffer. Next, 5 µL of SDS sample buffer was added to the beads, and the samples were boiled and then loaded onto 10% SDS-PAGE gels. Following protein transfer to nitrocellulose membrane (Amersham™ Protran™ 0.2 µm NC

Life Sciences), JNK and GSTP1 expression were detected by western blotting as described below.

Glutathione *S*-transferase activity assay

GST activity was measured using a GST fluorescent activity kit according to the manufacturer's protocol. Briefly, MIA PaCa-2 cells were treated with PL (0, 10, 100 µM) for 6 h. After 6 h, the cells were homogenized, centrifuged, and supernatant was collected for GST activity. The samples were placed into a 96-well plate with appropriate standards and controls. The fluorescence emission was read at 460 nm with excitation at 390 nm. The data represent the average ± standard deviation for three independent experiments.

Cell viability assay

MIA PaCa-2 and PANC-1 cells (4000/well) were seeded into 96-well plates. MIA PaCa-2 and PANC-1 cells were pre-treated with SP600125 or U0126 for 2 h and then treated with PL for 24 h. The cell viability was evaluated by adding 10 µL of 3-(4,5-dimethylthiazol-2-yl)-2,5-diphenyltetrazolium bromide (MTT) reagent to each well and incubating the plates for 3 h at 37 °C. MTT reagent was removed and DMSO (100 µl/well) was added to solubilize the crystals. The absorbance was measured at 570 nm using a xMark Microplate Spectrophotometer (BioRad).

Cytoplasmic and nuclear protein extraction

Cytoplasmic and nuclear protein extraction was performed as per the manufacturer's protocol (Thermo Scientific). Briefly, PDAC cells were harvested using trypsin and centrifuged to collect cell pellets. Cell pellets were re-suspended in cytoplasmic extraction reagent I (CERI), vortexed vigorously for 15 s, and CERII added, extracts vortexed again for 5 s and centrifuged at maximum speed (16,000×*g*). The supernatant was collected (cytoplasmic fraction) and the pellet re-suspended in nuclear extraction reagent (NER) and vortexed for 15 s, incubated for 10 min, repeated three times, and centrifuged at maximum speed to collect the nuclear fraction.

Western blotting

Total protein was isolated from the PDAC cell pellets using an SDS lysis buffer (Cell Signaling Technologies) containing protease and phosphatase inhibitors (Roche). Samples were briefly vortexed to dissociate cells. Forty µg of total protein isolated from vehicle control or treated cells were separated on 10% SDS–polyacrylamide gels at 100 V for 2 h. Proteins were transferred to nitrocellulose membranes at 100 V for 70 min at 4 °C. Blots were then probed overnight at 4 °C with primary antibodies. The next day, blots were rinsed with 1 × TBS-tween (0.1%) and probed with secondary antibody for 1 h at RT. The western blots were analyzed using SuperSignal West Femto Chemiluminescent Substrate (Thermo Fisher Scientific) and images were captured using the MultiImage™ Light Cabinet (Alpha Innotech). The expression level of p-JNK, p–c-Jun, p-ATF-2, p-ERK, cleaved caspase-3, cleaved PARP, c-Myc, HO-1, and Nrf-2 were normalized to total t-JNK, t-c-Jun, and t-ATF-2, t-ERK, β-actin, GAPDH, or histone H3 expression, respectively. Immunoblots were performed in triplicate, and the images in the figures represent one typical replicate. Densitometry was performed using Image J software according to our previously published manuscript [32].

RNA extraction

Total RNA was extracted from PDAC cells using an RNA isolation kit. Briefly, 350 µL of lysis solution was added to confluent cells. Cell lysates were transferred to microcentrifuge tubes and 200 µL of 100% ethanol was added. The tubes were vortexed vigorously for 10 s and clarified lysates with ethanol were transferred onto columns and centrifuged for 1 min. Next, 400 µL of wash solution was added and tubes were centrifuged for 1 min. This step was repeated three times. Afterwards, the columns were placed into fresh elution tubes, 30 µL of nuclease-free water was added to the columns, and the tubes were centrifuged at 200×*g* for 2 min followed by 12,000×*g* for 1 min at 4 °C.

Reverse transcription-quantitative polymerase chain reaction (RT-qPCR)

Total RNA was isolated from PDAC cell pellets (PANC-1 and MIA PaCa-2) using an RNA isolation kit as described above. One µg of total RNA was reverse transcribed into cDNA using the qScript cDNA synthesis kit, qScript reaction mix, and qScript reverse transcriptase (Quanta Biosciences). Steady-state mRNA levels of apoptosis and survival genes were determined for the cDNAs by reverse transcriptase quantitative polymerase chain reaction (RT-qPCR) using PrimePCR™ assays, Apoptosis and Survival Tier 1 H96, human, (Bio-Rad). The PCR reaction mix contained PrimePCR Assay (dried in well), SYBR Green Super mix (10 µL), cDNA (2 µL corresponding to the cDNA reverse transcribed from 10 ng RNA), and nuclease-free water (8 µL). The 96-well plate was then run on the MXpro 96 at 95 °C for 2 min, then 40 cycles of 95 °C for 5 s and 60 °C for 30 s. Data were processed and analyzed using PrimePCR™ Analysis Software provided by Bio-Rad (www.bio-rad.com/PrimePCR). The PrimePCR plates were run three times for three independent replicates. Furthermore, to validate *HO-1*, *CDKN1A*, *HSPA1A*, *MYC* levels,

primers were designed using Prime Express software (version 2.0; Applied Biosystems) and synthesized by Integrated DNA Technology or Sigma Aldrich, see Table 1 for primer sequences. A melt curve was done and one distinct peak was observed for all primer sets. The fold change in mRNA expression was calculated by comparing the 18S rRNA-normalized threshold cycle numbers (CT) in the ZnPP or PL-treated PDAC cells with those in the DMSO treated, or SP600125 + PL-treated PDAC cells, respectively. Duplicate wells were run for each experiment, and the experiments were performed in triplicate.

HO-1 knockout using CRISPR/Cas9

A HO-1 knock out cell line was created using the pSpCas9 BB-2A-GFP (Genescript, USA) vector, containing a single guide RNA (sgRNA) sequence (5′-TGGAGCGTCCGC AACCCGAC-3′), targeting HO-1. Transfections using

Table 1 RT-qPCR primer sequences

Gene name	Forward primer sequence	Reverse primer sequence
HO-1	AATTCTCTTGGCTGGCTTCCT	CATAGGCTCCTTCCTCCTTTCC
CDKN1A	GGACAGCAGAGGAAGACCATGT	GCCGTTTTCGACCCTGAGA
HSPA1A	CACCAAGCAGACGCAGATCTT	CAACAGATTGTTGTCTTTCGTCATG
MYC	GAAAAGGCCCCCAAGGTAGTT	TTTCCGCAACAAGTCCTCTTC

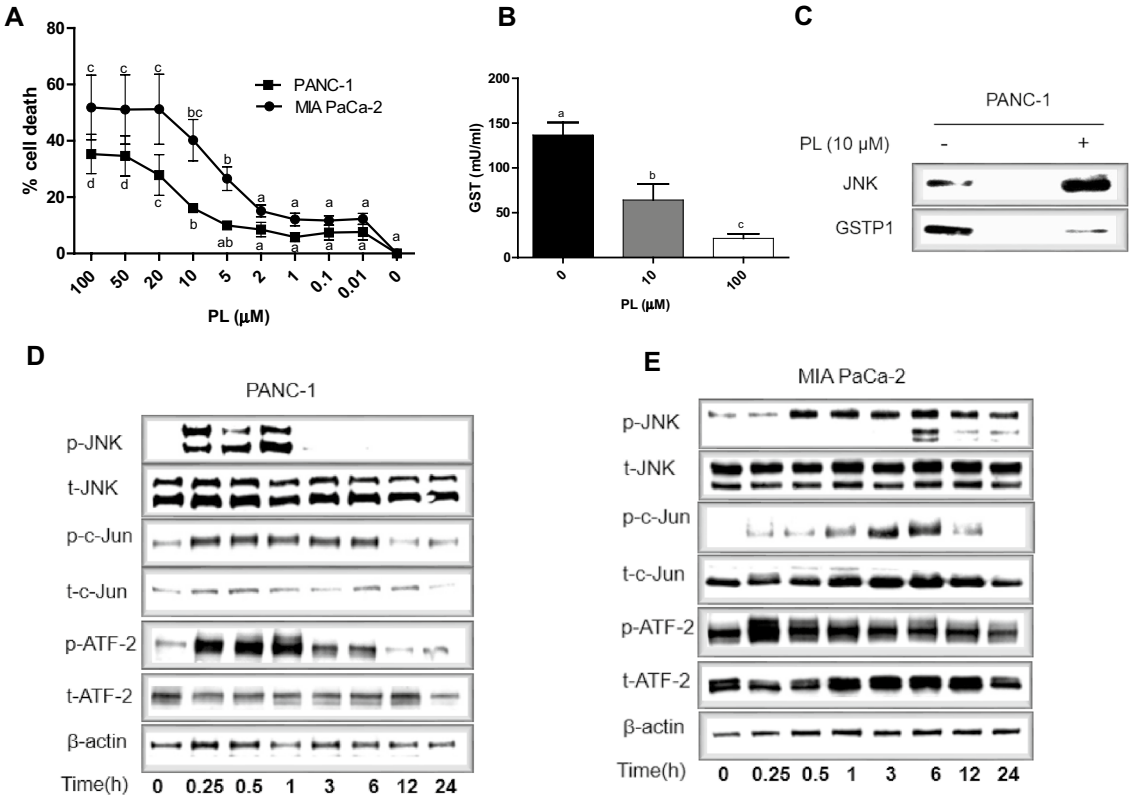

Fig. 1 Effect of PL on PDAC cell death, GST activity, and JNK signaling. **a** PANC-1 and MIA PaCa-2 cells were treated with PL (0–100 μM) for 72 h. The cell death percentages were analyzed by a CellTox Green assay. The data shown in the plot represent the average percent death relative to the vehicle-treated control ± SD for three independent experiments for both cell lines. Letters denote statistically significant differences in % cell death across treatment concentration ($p \leq 0.05$). **b** MIA PaCa-2 cells were treated with PL (0, 10 or 100 μM) for 6 h and GST activity was assessed via a GST activity fluorescent assay. The data shown in bar graph represent average GST activity (mU/mL) relative to vehicle treated-control ± SD for three independent replicates. Letters denote statistically significant differences ($p \leq 0.05$). **c** PANC-1 cells were treated with or without PL (10 μM) for 24 h. JNK protein complexes were pulled down using JNK-coated beads and western blotting for JNK and GSTP1 was done using western blotting. The experiment was performed at least three times, and the results shown above represent one typical experiment. **d** PANC-1 and **e** MIA PaCa-2 cells were treated with PL (10 μM) for 0–24 h. The phosphorylation of JNK and its effectors (c-Jun and ATF-2) were assessed using western blot. The experiment was repeated at least three times, and results shown above represent one typical experiment

Lipofectamine 2000 (Invitrogen, USA) were performed according to the manufacturer's instructions. Cells expressing high GFP were selected by single cell sorting into a 96-well plate containing media with antibiotics. Western blots for HO-1 were used to confirm knockout clones. Parent Capan-1 and HO-1 knockout cells were treated with different concentrations of PL and cultured for 48 h under hypoxia (4% oxygen) in a hypoxia chamber (Heracell VIOS 160i Tri-Gas CO2, Fisher, USA). Cell viability was measured by MTT assay (Promega, USA) as per manufacturer protocol.

Statistical analysis

Treatment estimates, standard errors, and significance were determined using fixed effects and mixed effects linear models. Where appropriate, model effects included treatment, gene, experiment, and experimental unit. All analyses were performed using the MIXED procedure in SAS software version 9.4 (SAS Institute, Cary NC).

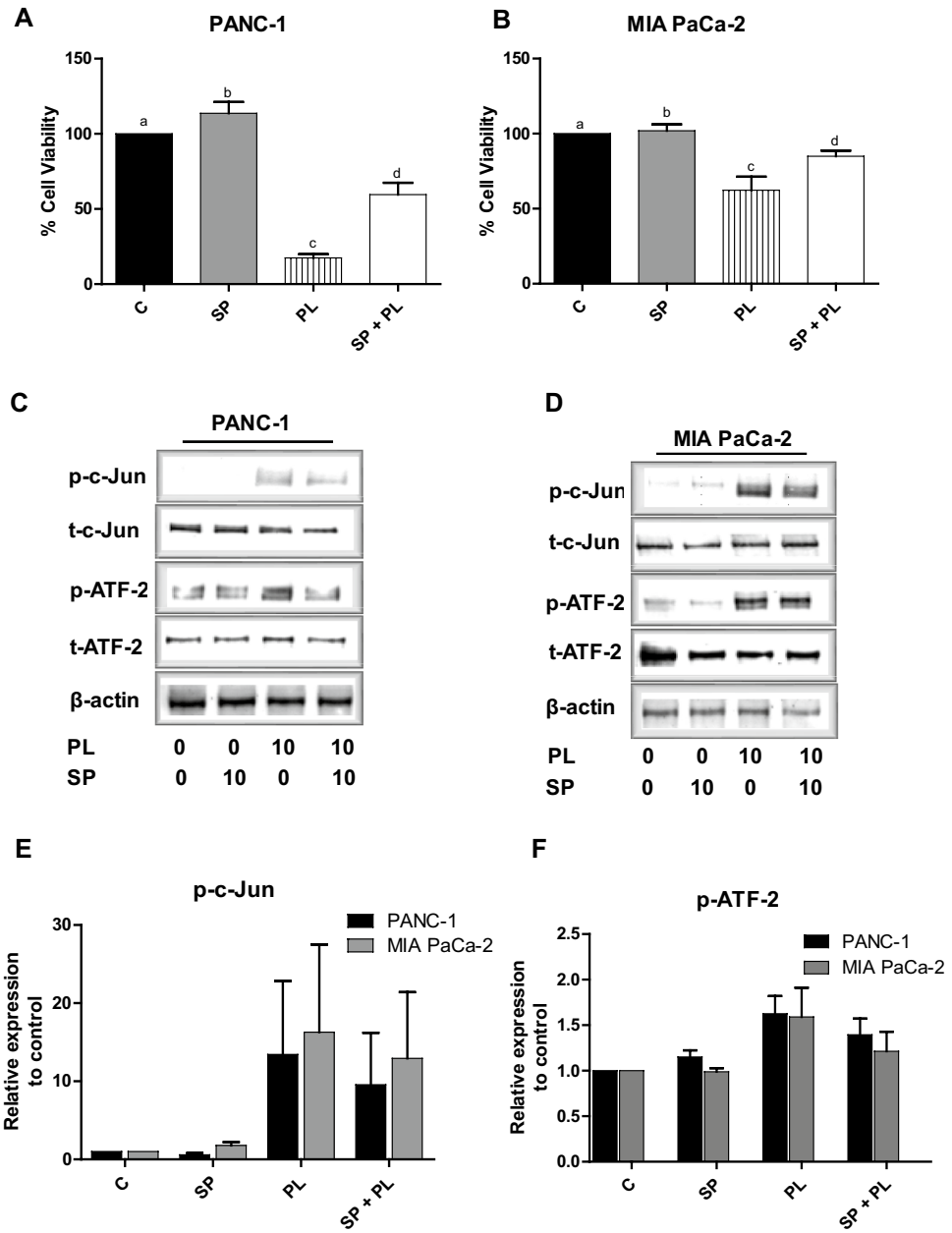

Fig. 2 JNK inhibition blocks PL-induced cell death and phosphorylation of JNK effectors in PDAC cells. **a** PANC-1 and **b** MIA PaCa-2 cells were treated with vehicle control (C), or pre-treated with SP600125 (SP; 10 μM) and then treated with PL (10 μM) for 48, and 24 h, respectively. The cell viability percentage were analyzed by MTT assay. The data shown in the bar graphs represent the average percent viability relative to the vehicle-treated control ± SD for three independent experiments for both cell lines. Treatments with bars that do not share a letter have differences that are statistically significant at $p \leq 0.05$. **c** PANC-1 and **d** MIA PaCa-2 were pre-treated with SP600125 (SP; 10 μM) for 2 h and then treated with PL (10 μM) for 3 h. The phosphorylation of c-Jun and ATF-2 were assessed using western blot. **e** p–c-Jun and **f** p-ATF-2 protein relative expression were quantified using Image J software. The experiment was repeated at least three times, and results shown above represent one typical experiment

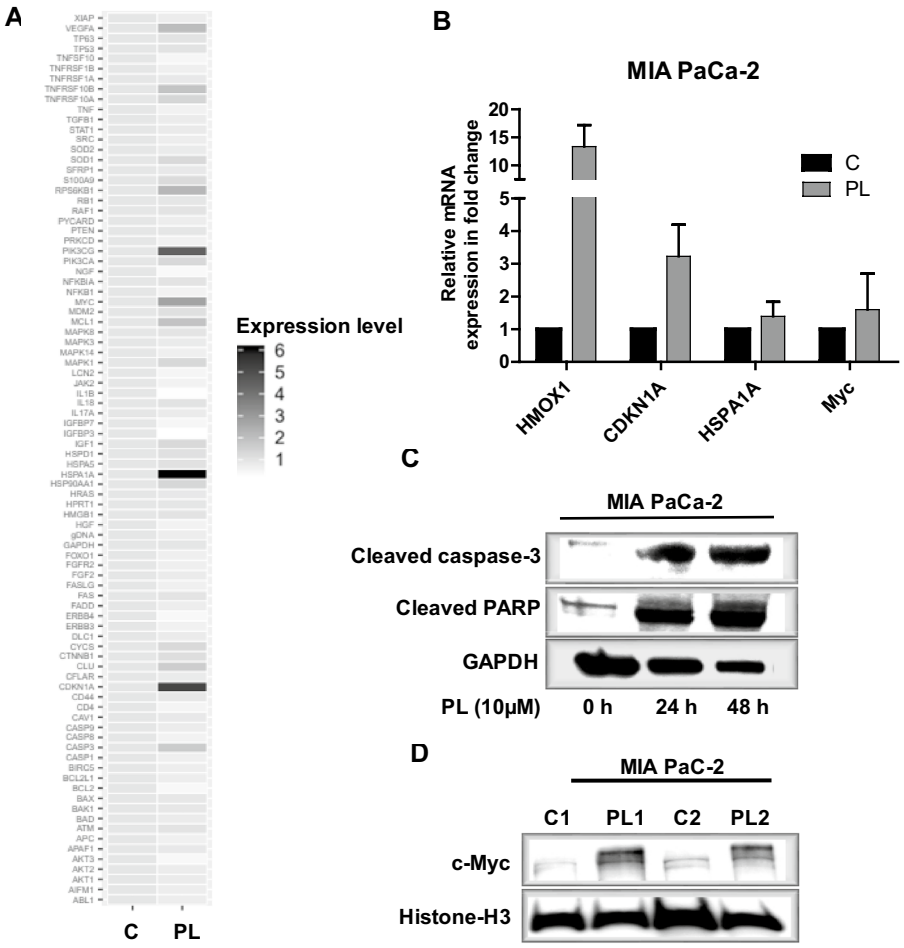

Fig. 3 PL induces expression of apoptosis-associated genes in PDAC cells. **a** The expression of apoptosis-related genes was assessed using apoptosis and survival pathway Tier 1 H96 plates in MIA PaCa-2 cells in response to PL (10 μM for 6 h) treatment, and heat map was generated using ggplot2 library in R. **b** Differentially expressed genes from the pathway plates were validated by RT-qPCR. The data shown in the bar graph represent fold change in mRNA expression in PL-treated relative to control-treated MIA PaCa-2 cells ± SD for three independent experiments. **c** MIA PaCa-2 were treated with PL (10 μM) for 24 and 48 h. The activation of caspase-3 and PARP were assessed using western blot. The experiment was repeated multiple times, and results shown above represent one typical experiment. **d** MIA PaCa-2 cells were treated with PL (10 μM) for 6 h. c-Myc expression was evaluated in the nuclear extracts for two replicate experiments: control (C1, C2) and PL-treated (PL1, PL2) cells. Histone-H3 expression was used to verify equal loading of nuclear extracts

Results

PL causes PDAC cell death in a concentration-dependent manner

Previously, we have shown PL reduces cell viability via inhibition of the cell cycle and cell proliferation in several pancreatic cancer cell lines both in vitro and in vivo [20, 33]. In this study, we used the CellTox™ Green assay to determine the effect of PL on MIA PaCa-2 and PANC-1 cell viability. The assay involves a fluorescent dye that binds to the DNA of dead or damaged cells. The two PDAC cell lines were treated with PL (0–100 μM) for 72 h and the percentage of cell death was determined. The results show that PL caused concentration-dependent cell death in both cell lines as compared to the DMSO-treated control (Fig. 1a). MIA PaCa-2 cells were more sensitive to PL than were PANC-1 cells with a 50% growth inhibitory (GI_{50}) concentration of 6.5 μM compared to 13.2 μM, respectively.

PL significantly decreases GST activity in PDAC cells in a concentration-dependent manner

Previous reports suggest PL increases ROS levels by binding to and inhibiting GSTP1 activity [33, 34]. Therefore, we determined if PL could inhibit global glutathione *S*-transferase (GST) activity in PDAC cells. We treated MIA PaCa-2 cells with PL (0, 10, or 100 μM) for 6 h and evaluated the activity of GST using a GST fluorescent activity kit. PL treatment of MIA PaCa-2 cells significantly ($p < 0.05$) decreased GST activity in a concentration-dependent manner with GST activity for 0, 10, or 100 μM PL being 166.7, 64.2, and 21.5 mU/mL, respectively (Fig. 1b).

PL reduced association of GSTP1 with JNK in PDAC cells

Previous reports have shown GSTP1/JNK dissociation can occur upon oxidative stress or direct binding of an inhibitor to GSTP1 [21, 22]. To determine if PL causes dissociation of JNK from GSTP1, we treated PANC-1 cells with PL (10 μM for 24 h) and pulled down JNK protein complexes via a co-immunoprecipitation assay. Western blotting for JNK and

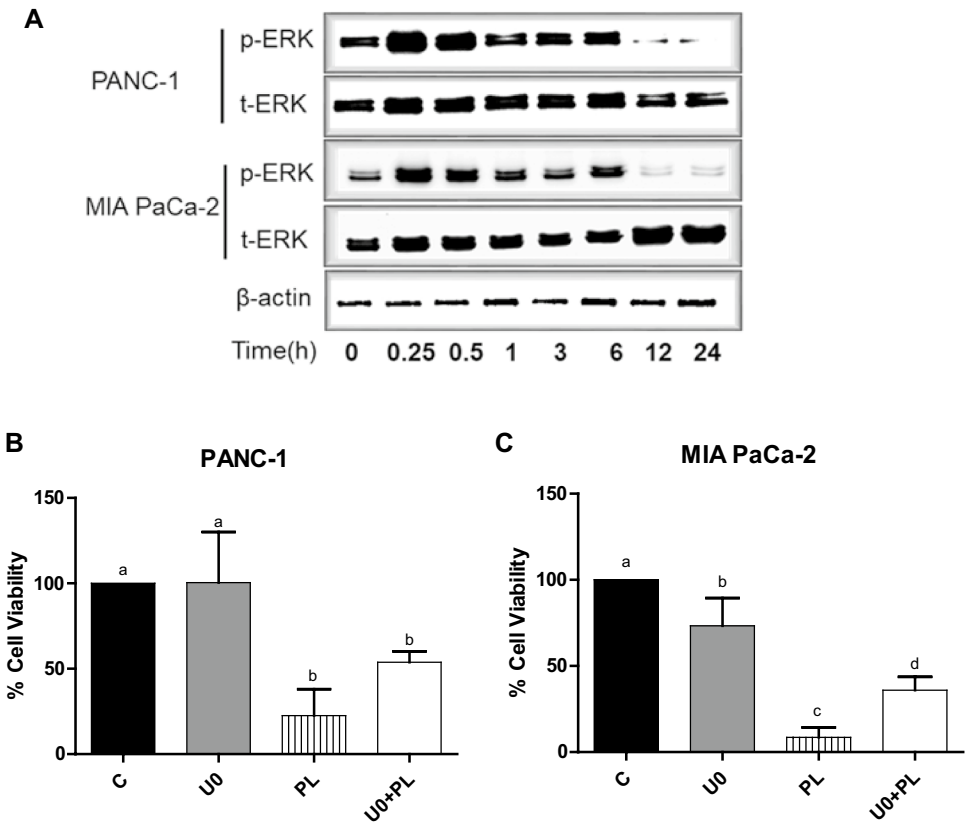

Fig. 4 PL treatment alters ERK signaling and MEK inhibition blocks PL-induced cell death in PDAC cells. **a** PANC-1 and MIA PaCa-2 were treated with PL (10 μM) for 0–24 h. The phosphorylation of ERK assessed using western blot. The experiment was repeated at least three times, and results shown above represent one typical experiment. **b** PANC-1 and **c** MIA PaCa-2 cells were treated with vehicle control (C), or pre-treated with U0126 (U0; 10 μM) for 2 h, PL (10 μM) for 24 h, or their combination. The cell viability percentages were analyzed by MTT assay. The data shown in the bar graphs represent the average percent viability relative to the vehicle-treated control ± SD for three independent experiments for both cell

GSTP1 was done for control and PL-treated cells. PL treatment resulted in the reduced association of GSTP1 with JNK (Fig. 1c). These data provide evidence the PL inhibits the interaction of GSTP1 and JNK, which could lead to JNK activation.

PL activates JNK signaling and its downstream effectors in PDAC cells

PL has been shown to activate JNK signaling in colon cancer cells [15]. To determine if PL also activates the JNK pathway in PDAC cells, we treated PANC-1 and MIA PaCa-2 cells with PL and evaluated the expression of phosphorylated JNK and two of its downstream effectors, c-Jun and ATF-2, via western blotting. PL treatment (10 μM for 0–24 h) of PDAC cells resulted in robust JNK activation within 15 min that diminished by 3 h in PANC-1 cells but remained elevated in MIA PaCa-2 cells (Fig. 1d, e). c-Jun and ATF-2 were also activated by PL treatment in both cell lines (Fig. 1d, e). c-Jun showed a more sustained activation in PANC-1 compared to MIA PaCa-2 cells; however, ATF-2 activation was more sustained in MIA PaCa-2 compared to PANC-1. These data indicate that PL treatment results in the activation of the JNK signaling pathway in PDAC cells.

JNK inhibition blocks PL-induced PDAC cell death

To determine if JNK is involved in PL-induced PDAC cell death, we used SP600125 to block JNK activation and determined the subsequent effect on PL-induced PDAC cell death. We pre-treated PANC-1 or MIA PaCa-2 cells with SP600125 (10 μM for 2 h) then treated cells with PL (10 μM) for 48 or 24 h, respectively, before analyzing cell viability using an MTT assay. Addition of SP600125 partially reversed the cytotoxic effects of PL for both PDAC cell lines (Fig. 2a, b). The percentage of viable cells following treatment with PL alone or SP600125 + PL was 17.45% vs. 59.61% for PANC-1 and 62.6% vs. 85.03% for MIA PaCa-2, respectively. We then determined if SP600125 could block PL-induced phosphorylation of JNK effectors (c-Jun and ATF-2). PANC-1 and MIA PaCa-2 cells were pre-treated with SP600125 (SP; 10 μM for 2 h) followed by PL treatment (10 μM for 3 h). Pre-treatment with SP600125 slightly, but insignificantly, blocked the phosphorylation of c-Jun and ATF-2 in both cell lines (Fig. 2c–f), which indicates additional signaling mechanisms other than JNK could activate c-Jun and ATF-2 in PL-treated cells.

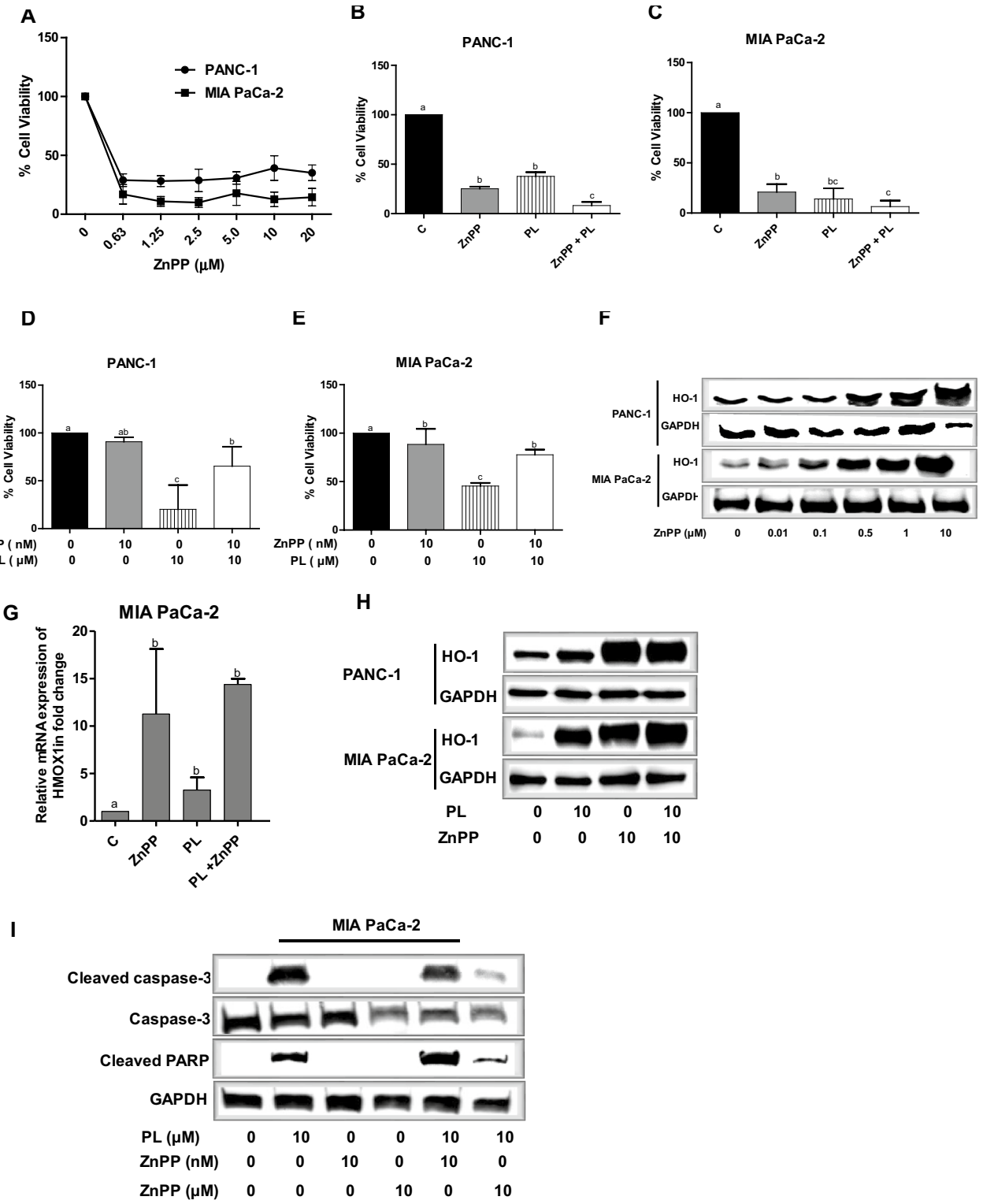

PL alters expression of apoptosis and cell survival-associated genes

To identify the mechanisms associated with PL-induced cell death, we used an apoptosis and survival pathway RT-qPCR plate to evaluate the effects of PL on gene expression in MIA PaCa-2 cells. MIA PaCa-2 cells were treated with PL (10 μM, for 6 h), RNA was isolated and gene expression was assessed using the RT-qPCR pathway plates. PL treatment of MIA PaCa-2 cells resulted in upregulation of a number of

◂**Fig. 5** Heme oxygenase-1 inhibition sensitizes PDAC cells to PL treatment. **a** PANC-1 and MIA PaCa-2 cells were treated with different concentration of ZnPP (0–20 μM). **b** PANC-1 and **c** MIA PaCa-2 cells were treated vehicle control (C) treated with ZnPP (10 μM) or PL (10 μM) for 24 h, or their combination. **d** PANC-1 and **e** MIA PaCa-2 cells were treated vehicle control (C) treated with ZnPP (10 nM) or PL (10 μM) for 24 h, or their combination. The cell viability percentage were analyzed by MTT assay. The data shown in the bar graphs represent the average percent viability relative to the vehicle-treated control ± SD for three independent experiments for both cell lines. Treatments with bars that do not share a letter have differences that are statistically significant at $p \leq 0.05$. **f** HO-1 protein expression in PDAC cells treated with ZnPP (0–10 μM) was determined using western blotting. PANC-1 and MIA PaCa-2 cells were treated with vehicle control (C), ZnPP (10 μM), PL (10 μM), or their combination for 24 h. **g** The mRNA expression of HMOX1 was assessed using RT-PCR. **h** HO-1 **i** Cleaved caspase-3 and cleaved PARP protein expression in PDAC cells treated with ZnPP or PL was determined using western blotting

genes including *HMOX1*, *HSPA1A, CASP3*, *CDKN1A*, *MYC*, and *PIK3CG* and downregulation of a number of genes including *BCL2*, *NFκB1*, *AKT3* genes (Fig. 3a). The largest fold change in gene expression was observed for *HMOX1* (31.7-fold increase). We validated the RT-qPCR plate results with our own primer sets (Supplemental Table 1). We confirmed PL elevates *HMOX1*, *CDKN1A*, *HSPA1A*, and *MYC* RT-qPCR (Fig. 3b). These results suggest PL alters expression of apoptosis and survival-associated genes.

PL causes apoptosis in MIA PaCa-2 cells

Previously, we reported that a caspase-3 inhibitor (zVAD-fmk) blocks PL-induced cell death in PANC-1 and MIA PaCa-2 cells [33]. Furthermore, previous reports have shown PL activates JNK signaling and results in apoptosis in various cancer cells [15, 16]. Therefore, to determine if PL induces apoptosis in PDAC cells, we treated MIA PaCa-2 cells with PL and evaluated the activation of caspase-3 and PARP via western blotting. PL treatment (10 μM for 24 and 48 h) of PDAC cells results in robust cleaved caspase-3 and cleaved PARP (Fig. 3c), suggesting apoptosis is induced in these cells by PL. To our surprise, we found that PL increased nuclear expression of c-Myc protein in PDAC cells (Fig. 3d).

PL alters ERK signaling in PDAC cells

The experiments above suggest that JNK is partially responsible for PL's cytotoxic effects in PDAC cells. Since ROS-induced ERK signaling is associated with reduced cell proliferation, and we have previously reported PL activates ERK signaling in colon cancer cells [18], we aimed to identify the effects of PL on ERK signaling. We treated PDAC cells (PANC-1 and MIA PaCa-2) with PL and evaluated the expression of phosphorylated ERK relative to total ERK. PL treatment (10 μM for 0–24 h) of PANC-1 or MIA PaCa-2 cells resulted in an initial ERK activation within 15 min that diminished by 3 h in both cell lines (Fig. 4a). However, at 12 and 24 h, phosphorylated ERK expression was reduced in both PL-treated PDAC cell lines. These results suggest PL leads to an early ERK signaling response that is ultimately suppressed over time.

ERK inhibition blocks PL-induced PDAC cell death

To determine if ERK signaling is involved in PL-induced PDAC cell death, we utilized a pharmacological MEK inhibitor (U0126) to block downstream ERK activation and determined the subsequent effect on PL-induced PDAC cell death. PANC-1 and MIA PaCa-2 were pre-treated with U0126 (10 μM for 2 h) then treated with PL (10 μM for 24 h). Cell viability was evaluated using an MTT assay. Addition of U0126 partially reversed the cytotoxic effects of PL for both PDAC cell lines (Fig. 4b, c). The percentage of viable cells following treatment with 10 μM PL alone or pre-treatment with 10 μM U0126 were 22.4% and 53.8% for PANC-1 and 8.6% and 35.9% for MIA PaCa-2, respectively (Fig. 4b, c).

Pharmacological inhibition of HO-1 yields mixed results in PDAC cells

HO-1 is an antioxidant enzyme frequently up-regulated in response to oxidative stress. However, there is some suggestion in literature that HO-1 can actually contribute to cell death [35]. To determine if the robust increase in HO-1 expression we observed in PL-treated cells was cytoprotective or cytotoxic, we used pharmacological inhibitors of HO-1 (zinc or tin protoporphyrin; ZnPP or SnPP) and determined the effect on PL-induced PDAC cell death. ZnPP was cytotoxic to PDAC cells at all concentrations tested (63 nM to 20 μM; Fig. 5a). Higher concentrations of ZnPP (10 uM) sensitized PDAC cells to PL treatment (Fig. 5b, c), while lower concentrations of ZnPP (10 nM) did not (Fig. 5d, e). ZnPP increased *HO-1* mRNA (Fig. 5f) and protein (Fig. 5g) expression alone and in combination with PL (Fig. 5h). Higher concentrations of ZnPP (10 μM) blocked PL-induced cleaved caspase-3 expression in PDAC cells, while lower concentrations of ZnPP (10 nM) did not (Fig. 5i).

SnPP (at high or low concentrations; 10 μM or 10 nM) is not cytotoxic to PDAC cells (Fig. 6a). SnPP partially blocks PL-induced cell death at both high (Fig. 6b, c) and low concentrations (Fig. 6d, e). Unlikely ZnPP, SnPP fails to induce HO-1 protein expression at 10 uM in PDAC cells (Fig. 6f). However, SnPP at low and high concentrations blocks PL-induced cleaved caspase-3 and PARP expression in PDAC cells (Fig. 6g). Collectively, these data suggest that non-toxic

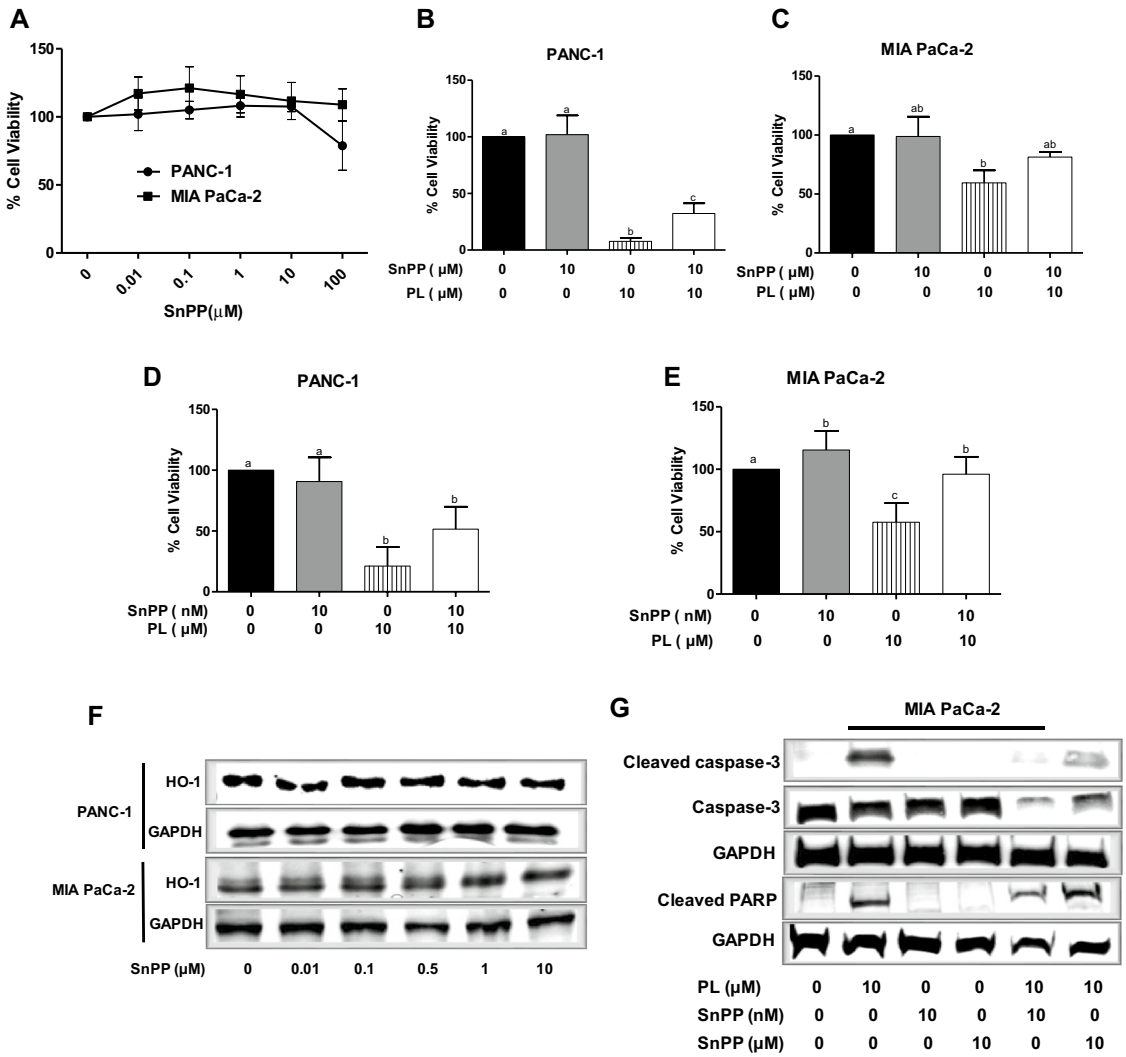

Fig. 6 Heme oxygenase-1 inhibition sensitizes PDAC cells to PL treatment. **a** PANC-1 and MIA PaCa-2 cells were treated with different concentration of SnPP (0–100 μM). **b** PANC-1 and **c** MIA PaCa-2 cells were treated vehicle control (C) treated with SnPP (10 μM) or PL (10 μM) for 24 h, or their combination. **d** PANC-1 and **e** MIA PaCa-2 cells were treated vehicle control (C) treated with SnPP (10 nM) or PL (10 μM) for 24 h, or their combination. The cell viability percentage were analyzed by MTT assay. The data shown in the bar graphs represent the average percent viability relative to the vehicle-treated control ± SD for three independent experiments for both cell lines. Treatments with bars that do not share a letter have differences that are statistically significant at $p \leq 0.05$. **f** HMOX1 protein expression in PDAC cells treated with SnPP (0–10 μM) was determined using western blotting. **g** MIA PaCa-2 cells were treated with vehicle control (C), ZnPP (10 nM, 10 μM), PL (10 μM), or their combination for 24 h. The expression of cleaved caspase-3 and cleaved PARP were determined using western blotting

concentrations of a HO-1 inhibitor protect PDAC cells from PL-induced cell death.

HO-1 knockout sensitizes PDAC cells to PL-induced cell death

Since ZnPP and SnPP experiments generated variable results at different concentrations,, we used CRISPR to knockout HO-1 and more definitively determine the role of HO-1 in PL-induced cell death. Western blotting showed complete loss of HO-1 expression in the knockout PDAC cells (Fig. 7a). HO-1 knockout cells were more sensitive to increasing concentrations of PL than parent cells under hypoxic conditions (Fig. 7b). These data demonstrate that HO-1 plays a role in protecting PDAC cells from PL-induced cell death in response to the enhanced stress signals the cells experience.

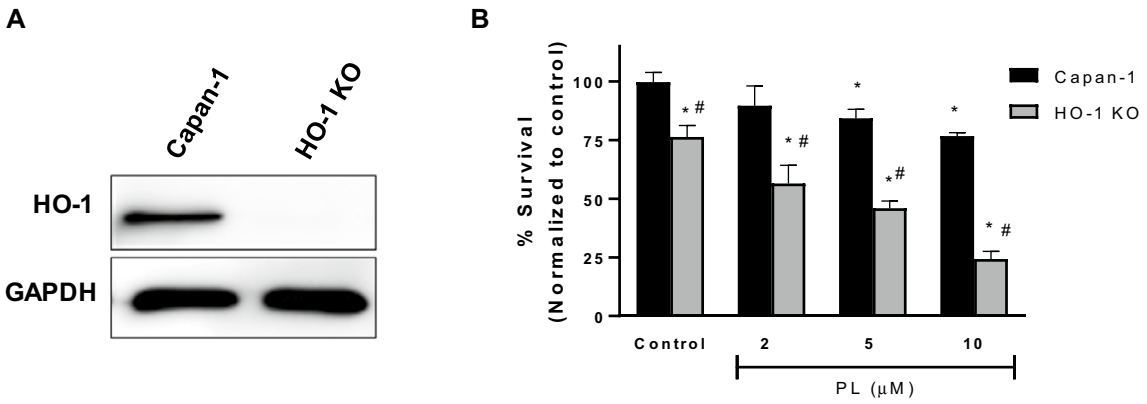

Fig. 7 Heme oxygenase-1 knockdown sensitizes PDAC cells to PL treatment. **a** Western blotting was done to confirm knockout of HMOX1 in Capan-1 cells. **b** Control and HMOX1 knockout Capan-1 cells were treated with PL (2, 5, and 10 μM) and cell viability was determined using MTT assays. The data shown in the bar graphs represent the average percent viability relative to the vehicle-treated control ± SD for three independent experiments for both cell lines. Treatments with bars that do not share a letter have differences that are statistically significant at $p \leq 0.05$

JNK inhibition blocks PL-induced nuclear translocation of Nrf2 and HMOX1 mRNA expression in PDAC cells

The results presented above showed PL activated JNK signaling and increased HO-1. To determine if PL-induced JNK signaling contributed to *HMOX1* expression, we evaluated the effect of the JNK inhibitor on *HMOX1* gene expression. JNK inhibition blocked PL-induced HMOX1 mRNA expression in PDAC cells (Fig. 8a). Since Nrf2 is the primary transcription factor regulating *HMOX1* mRNA expression, we then determined the effect of PL and JNK inhibition on Nrf2 nuclear localization. PL resulted in Nrf2 translocation to the nucleus (Fig. 8b), and JNK inhibition blocks PL-induced translocation to nucleus in PDAC cells (Fig. 8c). Collectively, these results suggest PL results in JNK activation, which leads to Nrf2 nuclear translocation and expression of *HMOX1* (Fig. 8d). In this context, increased *HMOX1* appears to be a compensatory response to the elevated stress levels encountered by PL treatment.

Discussion

PDAC is one of the most aggressive solid tumors with a 5-year survival rate of only 8% [36]. Understanding the mechanism(s) underlying the cytotoxic effects of an alternative therapy such as PL is essential for determining its therapeutic potential for PDAC. Our data demonstrate that PL induces PDAC cell death by activating MAPK signaling pathways and altering expression of apoptosis and survival-associated genes. We found that pharmacological inhibition of JNK or MEK inhibits PL-induced PDAC cell death. Further, PL treatment led to a large increase in HO-1 mRNA and protein expression, which when inhibited or knocked out resulted in greater toxicity to PDAC cells. These results indicate PL elicits an oxidative stress response mediated through MAPK pathways that leads to PDAC cell death, and at the same time, triggers a cytoprotective response that, if blocked, can increase PL's toxicity.

In our study, PL activates JNK signaling and its downstream-effectors, which results in increased expression of cleaved caspase-3 and cleaved PARP in PDAC cells, both hallmarks of apoptosis. Our results are in concordance with previous studies showing PL induces apoptosis via the JNK pathway in several cancer types, and JNK inhibition with N-acetyl-L-cysteine (NAC) or SP600125 blocks PL-induced ROS production and apoptosis [15–17, 37]. These reports suggest that JNK-signaling pathway might be a major mediator in PL-induced cancer cell death. Additionally, we observed PL affects ERK signaling in PDAC cells with an initial increase in ERK activation followed by decreased activity at 12 and 24 h. Previous studies have also reported PL induces ERK signaling at early time points (up to 1 [18] and 3 h [17]), and that PL induces cell death via ERK signaling in colon cancer cells [18] and ERK inhibition with U0126 blocked PL-induced apoptosis in cholangiocarcinoma cells [17]. Collectively, the results from our study along with previous reports demonstrate that JNK and ERK signaling are major mediators of PL-induced apoptosis in cancer cells.

Oxidative stress is enhanced in cancer cells relative to normal cells due to higher metabolic demands [38]. Consequently, cancer cells are more sensitive to therapies that perturb redox balance than are normal cells [39]. PL disrupts redox balance by inhibiting the phase II conjugating enzyme

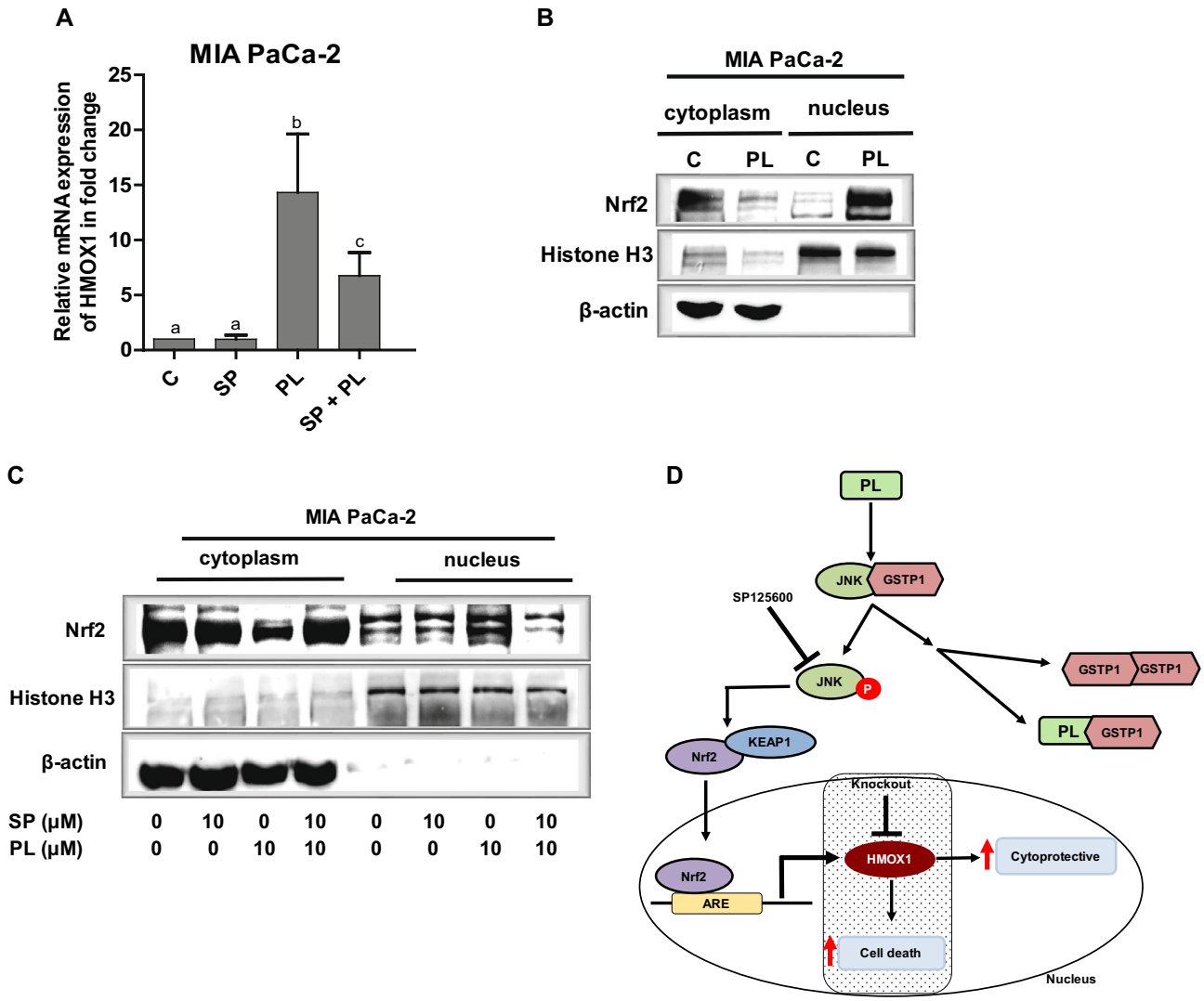

Fig. 8 JNK inhibition blocks PL-induced translocation of Nrf2 into nucleus in PDAC cells. **a** MIA PaCa-2 cells were treated with vehicle control (C) or pretreated with SP (10 μM) or U0 (10 μM) for 2 h and then treated with PL (10 μM) for 6 h. The mRNA expression of HMOX1 was assessed using RT-PCR. 18S rRNA was used to normalize the data. The data shown in the bar graphs represent mRNA expression in fold change relative to the vehicle-treated control ± SD for three independent experiments for both cell lines. Treatments with bars that do not share a letter have differences that are statistically significant at $p \leq 0.05$. **b** MIA PaCa-2 cells were treated with vehicle control (C) or PL (10 μM) for 6 h. **c** MIA PaCa-2 cells were treated with vehicle control (C) or pretreated with SP (10 μM) for 2 h and then treated with (10 μM) for 6 h. The expression of Nrf2 in cytoplasmic and nuclear protein extract was determined using western blotting. **d** Proposed mechanism for JNK-mediated PL-induced PDAC cell death

GSTP1 [34], which plays an important role in detoxification of electrophiles. We found PL treatment of PDAC cells resulted in reduced global glutathione *S*-transferase activity in PDAC cells. We also noted decreased association of GSTP1 with JNK when PDAC cells were treated with PL. It is possible that PL directly bound to GSTP1 to inhibit its interaction with JNK (Fig. 8d) [34]. It is also possible that PL directly increased ROS and the added oxidative stress resulted in GSTP1 dissociation from JNK and subsequent JNK signaling [21]. Either way, PL results in enhanced oxidative stress and MAPK signaling.

MAPK signaling activates transcription factors that influence gene expression to help mitigate redox imbalance. Under stress conditions, the transcription factors NFκB, Nrf2, and AP1 are all known to induce expression of phase II antioxidant enzymes such as HO-1 [40]. In this study, PL caused Nrf2 nuclear translocation which was associated with increased HO-1 mRNA and protein levels, and a JNK inhibitor blocked this response. In support of these results,

previous studies have shown a JNK inhibitor is able to block transcriptional activation of HO-1 [29].

The role of HO-1 in the stress response is widely thought to be cytoprotective [41]. HO-1 breaks down heme into three active products; carbon monoxide (CO), ferrous ions, and biliverdin, which is converted into the antioxidant bilirubin [42]. Among many functions, CO has antiproliferative and apoptotic properties which prevent tissue injury [43]. We used two different HO-1 inhibitors, ZnPP and SnPP, to determine if the HO-1 induced by PL is cytoprotective or cytotoxic. ZnPP, but not SnPP, was cytotoxic by itself, and a high concentration (10 μM) enhanced PL-induced PDAC cell death, suggesting a cytoprotective effect of HO-1. A low concentration (10 nM) of ZnPP or either concentration of SnPP blocked PL-induced cell death, suggesting a cytotoxic effect of HO-1. SnPP is less toxic than ZnPP and it is possible that the concentrations we tested did not actually inhibit HO-1 enzymatic activity. Indeed, we did not detect increased HO-1 protein in response to SnPP which is an indicator HO-1 may not have been inhibited. Further, we evaluated cell viability after 2 h of SnPP pretreatment and 24 h after PL treatment, which may have not been enough time to see a cytotoxic effect of the HO-1 inhibitor. Previous studies have reported similar results to ours indicating that SnPP alone does not affect cell proliferation, while ZnPP does [44]. The reduced cell proliferation was through decreased expression of cyclin D1 and independent of HO-1 expression [44, 45]. Similarly in our study, high concentration of ZnPP did not cause apoptosis (as evidenced by a lack of cleaved caspase-3 and PARP expression), but reduced cell viability in an MTT assay. Since we observed variable responses of HO-1 inhibitors on PDAC cell viability and markers of apoptosis, we utilized CRISPR/Cas9 technique to genetically inhibit HO-1 expression and evaluate its effect on PDAC cell viability. In our study, knockout of HO-1 enhanced PL-induced PDAC cell death, which suggests HO-1 serves a cytoprotective function in PDAC cells exposed to increased oxidative stress. In support of this, knockdown of HO-1 or its enzymatic inhibition with ZnPP sensitized pancreatic [46], myeloid leukemia [47], liver [48], hepatoma [49], and melanoma [50], cancer cells to chemotherapy or radiation. Our results are in contrast to a previously published report suggesting HO-1 played an important role in mediating PL-induced cell death [35]. The authors showed knockdown of HO-1 or its pharmacological inhibition blocked the ability of PL to induce apoptosis in human breast cancer cells (MCF7). The discrepancies could be due to differences in tumor type (breast vs. pancreatic), inhibitor concentration (unclear in the previous study), or cell culture conditions (hypoxic vs. normoxic conditions). These reports along with our data suggest that functional inhibition of HO-1 is a better method to elucidate the role of HO-1 in cancer.

In summary, we have identified new mechanisms by which PL induces PDAC cell death. Specifically, PL activates MAPK (JNK and ERK) signaling which leads to changes in gene expression and activation of apoptotic signaling (cleaved caspase and PARP) that induces PDAC cell death. Further, we have determined the robust increase in HO-1 due to PL treatment is a compensatory mechanism to try to protect cells from oxidative-stress induced cell death, as inhibition or knockout of HO-1 enhances the effects of PL. These results provide new insight into how PL influences PDAC cells and suggest altering the redox balance in PDAC cells is an effective therapeutic approach.

Acknowledgements We thank Jagadish Loganathan, Jeffrey Kittilson, and Megan Orr for their technical support and assistance. We would like to acknowledge the use of the Biostatistics Core Facility for statistical analysis in this manuscript. This study is funded by National Institute of General Medical Sciences of the National Institutes of Health, Award Number 1P20GM109024.

Funding NIH Grant number 1P20GM109024 (to KMR). Its contents are solely the responsibility of the authors and do not necessarily represent the official views of the NIH.

Compliance with ethical standards

Conflict of interest The authors declare no conflicts of interest.

References

1. Schaeffer HJ, Weber MJ (1999) Mitogen-activated protein kinases: specific messages from ubiquitous messengers. Mol Cell Biol 19(4):2435–2444
2. Pearson G, Robinson F, Beers Gibson T, Xu BE, Karandikar M, Berman K, Cobb MH (2001) Mitogen-activated protein (MAP) kinase pathways: regulation and physiological functions. Endocr Rev 22(2):153–183. https://doi.org/10.1210/edrv.22.2.0428
3. Davis RJ (2000) Signal transduction by the JNK group of MAP kinases. Cell 103(2):239–252
4. Zeke A, Misheva M, Remenyi A, Bogoyevitch MA (2016) JNK signaling: regulation and functions based on complex protein-protein partnerships. Microbiol Mol Biol Rev 80(3):793–835. https://doi.org/10.1128/MMBR.00043-14
5. Ventura JJ, Hubner A, Zhang C, Flavell RA, Shokat KM, Davis RJ (2006) Chemical genetic analysis of the time course of signal transduction by JNK. Mol Cell 21(5):701–710. https://doi.org/10.1016/j.molcel.2006.01.018
6. Mansouri A, Ridgway LD, Korapati AL, Zhang Q, Tian L, Wang Y, Siddik ZH, Mills GB, Claret FX (2003) Sustained activation of JNK/p38 MAPK pathways in response to cisplatin leads to Fas ligand induction and cell death in ovarian carcinoma cells. J Biol Chem 278(21):19245–19256. https://doi.org/10.1074/jbc.M208134200
7. Cobb MH, Goldsmith EJ (1995) How map kinases are regulated. J Biol Chem 270(25):14843–14846. https://doi.org/10.1074/jbc.270.25.14843
8. Garg TK, Chang JY (2003) Oxidative stress causes ERK phosphorylation and cell death in cultured retinal pigment epithelium:

prevention of cell death by AG126 and 15-deoxy-delta 12, 14-PGJ2. BMC Ophthalmol 3:5
9. Kim J, Wong PKY (2009) Oxidative stress is linked to ERK1/2-p16 signaling-mediated growth defect in ATM-deficient astrocytes. J Biol Chem 284(21):14396–14404. https://doi.org/10.1074/jbc.M808116200
10. Mebratu Y, Tesfaigzi Y (2009) How ERK1/2 activation controls cell proliferation and cell death is subcellular localization the answer? Cell Cycle 8(8):1168–1175. https://doi.org/10.4161/Cc.8.8.8147
11. Tang DM, Wu DC, Hirao A, Lahti JM, Liu LQ, Mazza B, Kidd VJ, Mak TW, Ingram AJ (2002) ERK activation mediates cell cycle arrest and apoptosis after DNA damage independently of p53. J Biol Chem 277(23):21110
12. Burotto M, Chiou VL, Lee JM, Kohn EC (2014) The MAPK pathway across different malignancies: a new perspective. Cancer 120(22):3446–3456. https://doi.org/10.1002/cncr.28864
13. Roh JL, Kim EH, Park JY, Kim JW, Kwon M, Lee BH (2014) Piperlongumine selectively kills cancer cells and increases cisplatin antitumor activity in head and neck cancer. Oncotarget 5(19):9227–9238. https://doi.org/10.18632/oncotarget.2402
14. Bezerra DP, Castro FO, Alves AP, Pessoa C, Moraes MO, Silveira ER, Lima MA, Elmiro FJ, Costa-Lotufo LV (2006) In vivo growth-inhibition of Sarcoma 180 by piplartine and piperine, two alkaloid amides from Piper. Braz J Med Biol Res 39(6):801–807. https://doi.org/10.1590/s0100-879X2006000600014
15. Li W, Wen CY, Bai HY, Wang XY, Zhang XL, Huang LL, Yang XL, Iwamoto A, Liu HL (2015) JNK signaling pathway is involved in piperlongumine-mediated apoptosis in human colorectal cancer HCT116 cells. Oncol Lett 10(2):709–715. https://doi.org/10.3892/ol.2015.3371
16. Li JH, Sharkey CC, King MR (2015) Piperlongumine and immune cytokine TRAIL synergize to promote tumor death. Sci Rep. 2:89. https://doi.org/10.1038/srep09987
17. Thongsom S, Suginta W, Lee KJ, Choe H, Talabnin C (2017) Piperlongumine induces G2/M phase arrest and apoptosis in cholangiocarcinoma cells through the ROS-JNK-ERK signaling pathway. Apoptosis 22(11):1473–1484. https://doi.org/10.1007/s10495-017-1422-y
18. Randhawa H, Kibble K, Zeng H, Moyer MP, Reindl KM (2013) Activation of ERK signaling and induction of colon cancer cell death by piperlongumine. Toxicol In Vitro 27(6):1626–1633. https://doi.org/10.1016/j.tiv.2013.04.006
19. Chen Y, Liu JM, Xiong XX, Qiu XY, Pan F, Liu D, Lan SJ, Jin S, Yu SB, Chen XQ (2015) Piperlongumine selectively kills hepatocellular carcinoma cells and preferentially inhibits their invasion via ROS-ER-MAPKs-CHOP. Oncotarget 6(8):6406–6421. https://doi.org/10.18632/oncotarget.3444
20. Dhillon H, Chikara S, Reindl KM (2014) Piperlongumine induces pancreatic cancer cell death by enhancing reactive oxygen species and DNA damage. Toxicol Rep 1:309–318. https://doi.org/10.1016/j.toxrep.2014.05.011
21. Wang T, Arifoglu P, Ronai Z, Tew KD (2001) Glutathione S-transferase P1-1 (GSTP1-1) inhibits c-Jun N-terminal kinase (JNK1) signaling through interaction with the C terminus. J Biol Chem 276(24):20999–21003. https://doi.org/10.1074/jbc.M101355200
22. Adler V, Yin Z, Fuchs SY, Benezra M, Rosario L, Tew KD, Pincus MR, Sardana M, Henderson CJ, Wolf CR, Davis RJ, Ronai Z (1999) Regulation of JNK signaling by GSTp. EMBO J 18(5):1321–1334. https://doi.org/10.1093/emboj/18.5.1321
23. Yin Z, Ivanov VN, Habelhah H, Tew K, Ronai Z (2000) Glutathione S-transferase p elicits protection against H2O2-induced cell death via coordinated regulation of stress kinases. Cancer Res 60(15):4053–4057
24. Ascione A, Cianfriglia M, Dupuis ML, Mallano A, Sau A, Tregno F, Pezzola S, Caccuri AM (2009) The glutathione S-transferase inhibitor 6-(7-nitro-2,1,3-benzoxadiazol-4-ylthio)hexanol overcomes the MDR1-P-glycoprotein and MRP1-mediated multidrug resistance in acute myeloid leukemia cells. Cancer Chemother Pharm 64(2):419–424. https://doi.org/10.1007/s00280-009-0960-6
25. Bauer M, Bauer I (2002) Heme oxygenase-1: redox regulation and role in the hepatic response to oxidative stress. Antioxid Redox Signal 4(5):749–758. https://doi.org/10.1089/152308602760598891
26. Dhillon H, Mamidi S, McClean P, Reindl KM (2016) Transcriptome analysis of piperlongumine-treated human pancreatic cancer cells reveals involvement of oxidative stress and endoplasmic reticulum stress pathways. J Med Food 19(6):578–585. https://doi.org/10.1089/jmf.2015.0152
27. Poss KD, Tonegawa S (1997) Reduced stress defense in heme oxygenase 1-deficient cells. Proc Natl Acad Sci USA 94(20):10925–10930. https://doi.org/10.1073/pnas.94.20.10925
28. Pileggi A, Cattan P, Molano RD, Berney T, Vizzardelli C, Fraker C, Oliver R, Ricordi C, Pastori R, Bach FH, Inverardi L (2001) Induced heme oxygenase-1 upregulation protects pancreatic beta cells from apoptosis in vitro. Sci World J 1:108. https://doi.org/10.1100/tsw.2001.125
29. Kietzmann T, Samoylenko A, Immenschuh S (2003) Transcriptional regulation of heme oxygenase-1 gene expression by MAP kinases of the JNK and p38 pathways in primary cultures of rat Hepatocytes. J Biol Chem 278(20):17927–17936. https://doi.org/10.1074/jbc.M203929200
30. Shan Y, Pepe J, Lu TH, Elbirt KK, Lambrecht RW, Bonkovsky HL (2000) Induction of the heme oxygenase-1 gene by metalloporphyrins. Arch Biochem Biophys 380(2):219–227. https://doi.org/10.1006/abbi.2000.1921
31. Gaitanaki C, Konstantina S, Chrysa S, Beis I (2003) Oxidative stress stimulates multiple MAPK signalling pathways and phosphorylation of the small HSP27 in the perfused amphibian heart. J Exp Biol 206(16):2759–2769. https://doi.org/10.1242/jeb.00483
32. Chikara S, Mamidi S, Sreedasyam A, Chittem K, Pietrofesa R, Zuppa A, Moorthy G, Dyer N, Christofidou-Solomidou M, Reindl KM (2018) Flaxseed consumption inhibits chemically induced lung tumorigenesis and modulates expression of phase II enzymes and inflammatory cytokines in A/J mice. Cancer Prev Res (Phila) 11(1):27–37. https://doi.org/10.1158/1940-6207.CAPR-17-0119
33. Mohammad J, Dhillon H, Chikara S, Mamidi S, Sreedasyam A, Chittem K, Orr M, Wilkinson JC, Reindl KM (2018) Piperlongumine potentiates the effects of gemcitabine in in vitro and in vivo human pancreatic cancer models. Oncotarget 9(12):10457–10469. https://doi.org/10.18632/oncotarget.23623
34. Harshbarger W, Gondi S, Ficarro SB, Hunter J, Udayakumar D, Gurbani D, Singer WD, Liu Y, Li L, Marto JA, Westover KD (2017) Structural and biochemical analyses reveal the mechanism of glutathione S-transferase Pi 1 inhibition by the anti-cancer compound piperlongumine. J Biol Chem 292(1):112–120. https://doi.org/10.1074/jbc.M116.750299
35. Lee HN, Jin HO, Park JA, Kim JH, Kim JY, Kim B, Kim W, Hong SE, Lee YH, Chang YH, Hong SI, Hong YJ, Park IC, Surh YJ, Lee JK (2015) Heme oxygenase-1 determines the differential response of breast cancer and normal cells to piperlongumine. Mol Cells 38(4):327–335. https://doi.org/10.14348/molcells.2015.2235
36. Siegel RL, Miller KD (2018) Jemal A (2018) Cancer statistics. CA: A Cancer J Clin 68(1):7–30. https://doi.org/10.3322/caac.21442
37. Xiong XX, Liu JM, Qiu XY, Pan F, Yu SB, Chen XQ (2015) Piperlongumine induces apoptotic and autophagic death of the

primary myeloid leukemia cells from patients via activation of ROS-p38/JNK pathways. Acta Pharmacol Sin 36(3):362–374. https://doi.org/10.1038/aps.2014.141
38. Sosa V, Moline T, Somoza R, Paciucci R, Kondoh H, LLeonart ME (2013) Oxidative stress and cancer: an overview. Ageing Res Rev 12(1):376–390. https://doi.org/10.1016/j.arr.2012.10.004
39. Liou GY, Storz P (2010) Reactive oxygen species in cancer. Free Radic Res 44(5):479–496. https://doi.org/10.3109/10715761003667554
40. Alam J, Cook JL (2007) How many transcription factors does it take to turn on the heme oxygenase-1 gene? Am J Respir Cell Mol Biol 36(2):166–174. https://doi.org/10.1165/rcmb.2006-0340TR
41. Gozzelino R, Jeney V, Soares MP (2010) Mechanisms of cell protection by heme oxygenase-1. Annu Rev Pharmacol Toxicol 50:323–354. https://doi.org/10.1146/annurev.pharmtox.010909.105600
42. Tenhunen R, Marver HS, Schmid R (1968) The enzymatic conversion of heme to bilirubin by microsomal heme oxygenase. Proc Natl Acad Sci USA 61(2):748–755. https://doi.org/10.1073/pnas.61.2.748
43. Loboda A, Jazwa A, Grochot-Przeczek A, Rutkowski AJ, Cisowski J, Agarwal A, Jozkowicz A, Dulak J (2008) Heme oxygenase-1 and the vascular bed: from molecular mechanisms to therapeutic opportunities. Antioxid Redox Signal 10(10):1767–1812. https://doi.org/10.1089/ars.2008.2043
44. La P, Fernando AP, Wang Z, Salahudeen A, Yang G, Lin Q, Wright CJ, Dennery PA (2009) Zinc protoporphyrin regulates cyclin D1 expression independent of heme oxygenase inhibition. J Biol Chem 284(52):36302–36311. https://doi.org/10.1074/jbc.M109.031641
45. Podkalicka P, Mucha O, Jozkowicz A, Dulak J, Loboda A (2018) Heme oxygenase inhibition in cancers: possible tools and targets. Contemp Oncol (Pozn) 22(1A):23–32. https://doi.org/10.5114/wo.2018.73879
46. Berberat PO, Dambrauskas Z, Gulbinas A, Giese T, Giese N, Kunzli B, Autschbach F, Meuer S, Buchler MW, Friess H (2005) Inhibition of heme oxygenase-1 increases responsiveness of pancreatic cancer cells to anticancer treatment. Clin Cancer Res 11(10):3790–3798. https://doi.org/10.1158/1078-0432.CCR-04-2159
47. Zhe N, Wang J, Chen S, Lin X, Chai Q, Zhang Y, Zhao J, Fang Q (2015) Heme oxygenase-1 plays a crucial role in chemoresistance in acute myeloid leukemia. Hematology 20(7):384–391. https://doi.org/10.1179/1607845414Y.0000000212
48. Sass G, Leukel P, Schmitz V, Raskopf E, Ocker M, Neureiter D, Meissnitzer M, Tasika E, Tannapfel A, Tiegs G (2008) Inhibition of heme oxygenase 1 expression by small interfering RNA decreases orthotopic tumor growth in livers of mice. Int J Cancer 123(6):1269–1277. https://doi.org/10.1002/ijc.23695
49. Liu YS, Li HS, Qi DF, Zhang J, Jiang XC, Shi K, Zhang XJ, Zhang XH (2014) Zinc protoporphyrin IX enhances chemotherapeutic response of hepatoma cells to cisplatin. World J Gastroenterol 20(26):8572–8582. https://doi.org/10.3748/wjg.v20.i26.8572
50. Frank J, Lornejad-Schafer MR, Schoffl H, Flaccus A, Lambert C, Biesalski HK (2007) Inhibition of heme oxygenase-1 increases responsiveness of melanoma cells to ALA-based photodynamic therapy. Int J Oncol 31(6):1539–1545